Title

Electron Spectroscopy and Computational Studies of Dimethyl Methylphosphonate.

Journal

The Journal of Physical Chemistry A, 120(12)

ISSN

1089-5639

Authors

Head, Ashley R

Tsyshevsky, Roman

Trotochaud, Lena

et al.

Publication Date

2016-03-31

DOI

10.1021/acs.jpca.6b01098

Peer reviewed

Electron Spectroscopy and Computational Studies of Dimethyl Methylphosphonate

Ashley R. Head,[1] Roman Tsyshevsky,[2] Lena Trotochaud,[1] Bryan Eichhorn,[3] Maija M. Kuklja,[,2]*

Hendrik Bluhm[1,]*

[1] Chemical Sciences Division, Lawrence Berkeley National Laboratory, Berkeley, CA 94720

[2] Materials Science and Engineering Department and [3] Department of Chemistry and Biochemistry, University of Maryland, College Park, MD 20742

Abstract

Dimethyl methylphosphonate (DMMP) is one of the most widely used molecules to simulate chemical warfare agents in adsorption experiments. However, the details of the electronic structure of the isolated molecule have not yet been reported. We have directly probed the occupied valence and core levels using gas phase photoelectron spectroscopy and the unoccupied states using near-edge X-ray absorption fine structure (NEXAFS) spectroscopy. Density functional theory (DFT) calculations were used to study the electronic structure, assign the spectral features, and visualize the molecular orbitals. Comparison with parent molecules shows that valence and core level binding energies of DMMP follow trends of functional group substitution on the P center. The photoelectron and NEXAFS spectra of the isolated molecule will serve as a reference in studies of DMMP adsorbed on surfaces.

Introduction

Molecules with an organophosphonate structure, P(O)(OR)(OR')(R''), garner interest for uses in a wide variety of fields, including tuning energy levels at semiconductor device interfaces,[1] as corrosion inhibitors,[2] and as pesticides and herbicides.[3] They also exhibit a range of toxicity to animals; some of the most infamously noxious molecules contain phosphonate functional groups and are used as chemical warfare agents (CWAs).[3] With the ever-present threat posed by CWAs, there is an acute need for new materials for uses in sensors, personal protection equipment, and degradation catalysts, all of which require an understanding of the electronic structure and reactivity of this class of molecules. However, due to personnel safety concerns, simulant molecules are used in experimental studies, with dimethyl methylphosphonate (DMMP), $P(O)(OCH_3)_2(CH_3)$, being one of the most common. Full details of the electronic structure of DMMP have not been reported, and a careful study of DMMP in the gas phase (i.e. without intermolecular interactions, solvation effects, and other condensed phase effects) is needed. Reference gas-phase photoelectron and X-ray absorption spectra, which provide information about occupied and unoccupied molecular states, respectively, will aid in the interpretation of future studies of DMMP interactions with solids and liquids.

CWA simulants offer clear advantages in terms of experimental safety but suffer the disadvantage of an incomplete understanding of the actual CWA molecules due to removal of a key functional group. While DMMP retains the phosphoryl oxygen, methyl group, and alkoxide moieties of the G-type and V-type nerve agents (the most common classes of CWAs), the P-F or P-S-R group is missing (cf. Figure 1).[3] Computational chemistry can provide the link between simulant molecules and real CWAs. Comparing computed energies with those measured in gas-phase electron spectroscopy experiments can validate theoretical results and guide further experiments. In turn, theory can predict properties of real CWAs. Quantum chemical calculations have been employed recently mainly to explore gas-phase decomposition mechanisms of DMMP[4,5] and to simulate adsorption and decomposition of DMMP and real agents (Sarin and VX) on various oxides,[6-11] carbon nanotubes,[12] and graphene.[13]

The electronic structure of DMMP is also interesting from a basic spectroscopy perspective. The gas-phase electronic structures of simple phosphines (PR_3), phosphites [$P(OR)_3$], and phosphates [$P(O)(RO)_3$] have been studied previously with semi-empirical[14,15] and quantum chemical calculations[16] and both valence[16-18] and core level[14,19-21] photoelectron spectroscopy. Correlations between binding energies and functional groups have been established.[14,15] More complex P-containing molecules have been investigated to a lesser extent, and thus, a thorough study of DMMP offers the opportunity to experimentally assess these correlations. The gas-phase valence photoelectron spectrum of DMMP was measured previously;[18] however, due to poor resolution, peak assignments were difficult. The gas-phase near-edge X-ray absorption fine-structure (NEXAFS) spectra of DMMP have not been reported so far but can aid in the identification of condensed phase effects, such as intermolecular interactions and hydrogen bonding.[22,23]

Here, we present the valence photoelectron spectrum of DMMP together with peak assignments based on DFT calculations. The gas-phase core-level spectra (P 2p, C 1s, O 1s) are also presented and compared with spectra of related molecules in the literature to illustrate systematic binding energy shifts with functional group substitutions on the central P atom. NEXAFS spectra of the C and O K-edges are interpreted with the aid of DFT calculations. Together, these results encompass a detailed description of the electronic structure of DMMP and serve as a benchmark for more complex spectroscopic and computational studies of DMMP, other simulants, and CWAs.

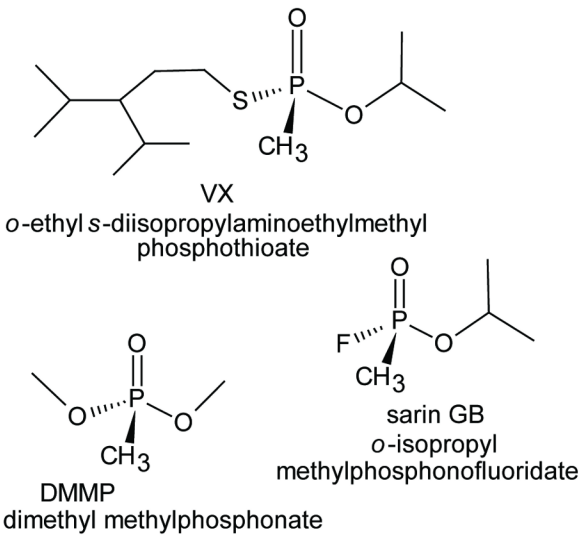

Figure 1. The molecular structure of selected CWAs in the V-series (VX) and G-series (sarin GB). DMMP is used as a simulant for both of these CWAs.

Experimental

Photoelectron and X-ray Absorption Spectroscopy

The photoelectron and NEXAFS spectra were collected at the ambient pressure X-ray photoelectron spectroscopy end station[24] at beamline 11.0.2[25] at the Advanced Light Source at Lawrence Berkeley National Laboratory. Dimethyl methylphosphonate (>97%, Fluka) was degassed via freeze-pump-thaw cycles and introduced into the high pressure analysis chamber of the spectrometer via a leak valve. The DMMP pressure during the measurements was 0.08 Torr. Oxygen gas was introduced into the analysis chamber (0.07 Torr) to calibrate the binding energy scale to the vacuum level at infinity (VL_∞) via the $^4\sum_u^-$ line of O 2s ionization (24.58 eV)[26,27] for the valence spectrum and the $^4\sum^-$ line of the O 1s ionization (543.37 eV)[27] for the core levels. The core level C 1s, O 1s and P 2p spectra were collected with an incident photon energy of 735 eV, and the valence band data were collected with a photon energy of 275 eV. The combined spectrometer and beamline resolution was better than 0.3 eV. Polynomial backgrounds were

subtracted from the photoelectron spectra. The peaks were fit with asymmetric Gaussian functions,[28] and the error in the binding energies is estimated to be ±0.05 eV. The NEXAFS data were collected in partial electron yield mode. The O K-edge was collected with a kinetic energy of 440 eV and a 20 eV kinetic energy bandwidth, and the C K-edge was collected with 220 eV kinetic energy and 10 eV bandwidth. The NEXAFS data were corrected for I_0 by subtracting the spectrum of clean Au foil. The photon energy scale was calibrated by the energy difference between first and second order photons.

Computational Details

The molecular and electronic structure of DMMP was studied with Gaussian 09 computer suite.[29] The valence spectrum of DMMP was assigned using one-electron energies of Kohn-Sham orbitals obtained with the M06-2X[30] functional and 6-31+G(d,p) basis set. Total densities of states (DOS) and partial densities of states (PDOS) projected on each atom of DMMP were calculated using the GaussSum code[31]. The X-ray absorption spectrum was calculated using time-dependent density functional theory (TD-DFT)[32] with the BP86[33,34] functional and the TZVP[35,36] basis set as implemented in ORCA[37] package. Only excitations from the localized O and C 1s orbitals have been taken into consideration.[38,39]

DMMP is known to have three conformers which differ in the relative dihedral angles of the CH_3-O-P groups.[40] We have presented calculation results of the experimentally observed lowest energy conformer[40] (Figure S1, Table S1). The two lowest energy conformers were found to be nearly isoenergetic with essentially no energetic barrier between them. Calculations revealed nearly identical electronic properties of these two configurations. The third conformer is not likely to contribute to the spectra due to the high barrier of internal rotation. Calculated valence and NEXAFS spectra of this conformer are slightly different in energy spacing but do not change the spectral assignments presented here. This analysis of the conformers is in agreement with a previously published gas phase spectroscopy and computational study.[40] Calculated valence and NEXAFS spectra of all conformers are presented in the Supporting Information.

Results and Discussion

Core-level binding energies

As part of the electronic structure characterization of DMMP in the gas phase, core-level photoelectron spectra were collected and compared with those of similar molecules published previously. The P 2p, C 1s, and O 1s photoelectron spectra are shown in Figure 2. The asymmetry on the high binding energy side of the peaks is due to vibrational broadening. The spin-orbit components in the P 2p spectrum are well-resolved with a splitting of 0.85 eV. In the C 1s spectrum (Fig. 2b), the binding energy of the methyl group is 291.0 eV and that of the methoxy groups is 292.7 eV. In the O 1s spectrum, the peak at 536.5 eV is assigned to the phosphoryl oxygen and the peak at 538.9 eV to the methoxy groups. The peak areas in both the C 1s and O 1s spectra have the expected 2:1 area ratio based on the stoichiometry of the intact molecule and chemical degeneracy of the methoxy groups. Calculated one-electron Kohn-Sham orbital energies corresponding to C 1s, O 1s, and P 2p core levels correctly reproduce experimental trends (Table 1). Quantitatively, the calculated values agree with the experiments within 1.3%.

Core level ionization energies of DMMP are compared to those of similar molecules in the literature to demonstrate correlations between binding energy shifts and functional groups on the P center. Table 1 lists binding energies for DMMP (this work), trimethyl phosphine oxide [$P(O)(CH_3)_3$][19,20] and trimethyl phosphate [$P(O)(OCH_3)_3$].[21] Replacing a methoxy group with a methyl group lowers the P 2p binding energy by about 0.7 eV per methyl group, according to the binding energies in Table 1. DMMP follows this pattern with the P $2p_{3/2}$ binding energy 0.8 eV lower than that of $P(O)(OCH_3)_3$. This trend reflects the electronegativity of the functional groups; the more electronegative oxygen reduces the amount of electron density on the P atom, in turn increasing the P 2p binding energy. This trend is also seen in the O 1s binding energy of the phosphoryl oxygen, where replacing a methoxy group with a methyl group results in about a 0.2

eV decrease. The C 1s and O 1s binding energies of the methyl and methoxy substituents do not vary much among these three molecules.

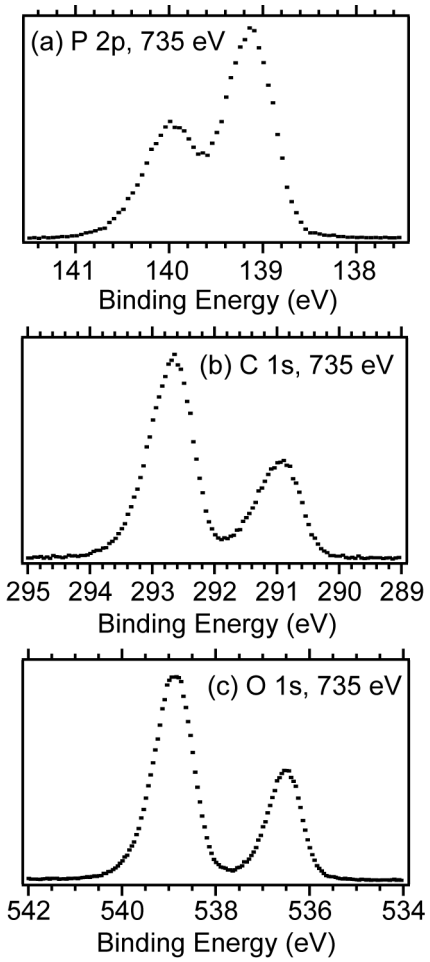

Figure 2. Gas-phase core level photoelectron spectra of the (a) P 2p, (b) C 1s, and (c) O 1s core levels of DMMP, collected with a photon energy of 735 eV.

Table 1. P 2p, C 1s, and O 1s ionization energies of DMMP and related molecules in the literature. Calculated core ionization energies of DMMP are also given. All values are in eV.

				DMMP	
		$P(O)(CH_3)_3$[a]	$P(O)(OCH_3)_3$[b]	Exp.	Calc.
P $2p_{3/2}$		137.8	139.9[c]	139.1	138.4
C 1s	P-CH_3	290.7		291.0	287.4
	P-OCH_3		292.7	292.6	288.6
O 1s	P=O	536.1	536.7	536.5	533.4
	P-OCH_3		539.1	538.9	535.5

a Ref. [19], [20]
b Ref. [21]
c The spin-orbit components could not be resolved, thus this value is an average of the $2p_{3/2}$ and $2p_{1/2}$ components.

Occupied Molecular Orbitals

Figure 3a shows the valence spectrum collected using a 275 eV photon energy and a fit of the spectrum with asymmetric Gaussian components.[28] Due to the changes in the photoionization cross sections between the 275 eV photon energy used here and the He I source (21.22 eV) used in the previous study,[18] the intensity profile of the spectrum is different. However, the vertical (IE_{vert}, HOMO ionization) and adiabatic ionizations (IE_{ad}, estimated from the onset of the first ionization[41]) match the literature values, as shown in Table 2. Calculated energies are compared to experimental values in Table 2 and are found to agree well, indicating that the theory is accurately modelling the electronic structure. The IE_{vert} is calculated by comparing the energy of the neutral molecule with the cation in the same geometry, and the IE_{ad} is the energy difference between the neutral molecule and the cation in the optimized geometry. The relaxation energy of the cation (λ) is the difference between these two energies. The vertical black lines in Figure 3b indicate the energy of the Kohn-Sham orbitals and correlate well with the peak positions, resulting in the peak assignments in Table 3, which shows also the binding energies and fit parameters. Symmetry-allowed mixing of the molecular orbitals complicates the spectrum in comparison to simpler phosphites that lack a phosphoryl oxygen.

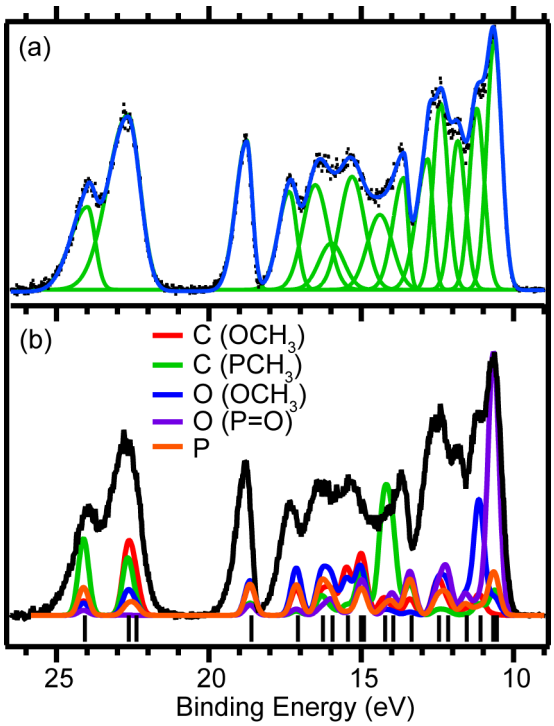

Figure 3. (a) Valence spectrum of DMMP (dots) measured using a photon energy of 275 eV and a fit (blue line) of asymmetric Gaussian functions (green lines). (b) Comparison of the valence spectrum shown in (a) (black line) with the PDOS of the methoxy carbon (red), methyl carbon (green), methoxy oxygen (blue), phosphoryl oxygen (purple), and the phosphorus (orange). The DOS are normalized such that the height of the phosphoryl oxygen DOS matches that of the HOMO ionization at ~10.5 eV. The energy scale of the DOS has been shifted by 0.84 eV to be aligned with the HOMO ionization. The black vertical lines are calculated Kohn-Sham orbital energies and have not been shifted.

Table 2. Relevant energies of DMMP from the experiment, calculations, and literature. All values are in eV.

	Experiment	Literature[a]	Calc.[b]
IE_{ad}	10.00	10.00[c]	9.77
IE_{vert}	10.64	10.71	10.60
λ	0.64	0.71	0.83

[a] Ref. [18]
[b] Calculated using M06-2X/6-31+G(d,p) level of theory
[c] Estimated from the onset of the first ionization energy in the reported spectrum

Table 3. The binding energies, Gaussian full-widths at half maximum (FWHM), and peak areas of the fit of the valence spectrum of DMMP. Binding energies and widths are in eV. Peak areas are in arbitrary units and normalized to the first peak.

Peak	Binding Energy	FWHM, high BE	FWHM, low BE	Area	Molecular orbital character[a] (major, *minor* contributions)
1[b]	10.64	0.56	0.56	100	LP(P=O), *LP(OCH_3)*
2	11.21	0.56	0.56	73	LP(P-OCH_3), *LP(P=O)*
3	11.83	0.56	0.56	60	LP(P-OCH_3) , *LP(P=O)*
4	12.40	0.56	0.56	75	σ(P=O)
5	12.82	0.87	0.40	59	π(P=O)
6	13.61	0.83	0.34	47	σ(P-CH_3), σ(P=O)
7	14.39	0.96	0.96	52	
8	15.30	0.96	0.96	78	
9	15.98	0.96	0.96	32	σ(P-O),σ(C-H), σ(C-O)
10	16.51	0.96	0.96	72	
11	17.36	0.86	0.57	50	
12	18.76	0.84	0.37	65	σ(P(3s)-OCH_3), *O 2s(P=O)*
13[b]	22.66	1.56	0.94	157	C 2s, *σ(P-OCH_3)*
14	23.98	1.33	0.58	57	C 2s, *σ(P-CH_3), σ(P-OCH_3)*

[a] LP = lone pare of electrons
[b] These Gaussian functions represent the ionization of two molecular orbitals.

The HOMO of phosphine oxides ($P(O)R_3$) is doubly degenerate and mostly consists of the oxygen lone pair of the phosphoryl oxygen.[17] Replacing the alkyl groups with alkoxide groups

adds an interaction of the phosphoryl lone pair with those of the O atom in the alkoxide groups.[17,18] In DMMP, this interaction is seen in the HOMO and HOMO-1 molecular orbital plots in Figure 4. The first ionization in the spectrum is assigned to these orbitals as the energy separation between them cannot be experimentally resolved. Figure 3b overlays the valence spectrum with the calculated PDOS projected onto each atom and shows that the first ionization is largely of P=O character. Analogous to the core level ionizations, the stabilizing effect of the methoxy groups on the HOMO ionization is seen in the trend of the IE_{vert} with that of DMMP (10.64 eV) falling between $P(O)(CH_3)_3$ at 9.90 eV[16,17] and $P(O)(OCH_3)_3$ at 10.90 eV.[18]

The molecular orbitals of DMMP (virtual C_s symmetry) can be related to the two parent molecules $P(O)(CH_3)_3$ and $P(O)(OCH_3)_3$ that have C_{3v} symmetry, as illustrated in the correlation diagram of their ionization energies in Figure 5. Phosphates have three molecular orbitals based on the lone pairs of electrons on the O atoms in the alkoxide groups: $1a_2$ and $4e$.[18] Since DMMP has only two methoxide groups, the $1a_2$ disappears and the *4e* orbitals split to *31a'* and *30a''*, the the HOMO-2 and HOMO-3, respectively. These molecular orbitals also have some symmetry-allowed interaction with the phosphoryl oxygen (cf. Figure 4). The peak at 12.40 eV is assigned to the HOMO-4, mostly the phosphoryl σ bond. The phosphoryl π bond (HOMO-5) has a larger binding energy at 12.82 eV. Overall, these molecular orbital ionizations are at lower energies than the analogous orbitals in the parent $P(O)(OCH_3)_3$[18] (cf. Figure 5), reflecting the replacement of one methoxy group with a less electronegative methyl group. The binding energy range 14.2 – 17.4 eV contains several overlapping ionizations corresponding to σ(C-H), σ(P-O) and σ(C-O), and no direct assignments are attempted; the Gaussian functions used in this region are for intensity only and do not represent specific molecular orbitals. The DOS from DFT calculations allows for the assignment of the three highest binding energy peaks that were not seen in the previously reported spectrum.[18] The separate peak at 18.76 eV is from the HOMO-15, a molecular orbital with contributions from the P 3s atomic orbital and σ(C-O) orbitals. The peak at 22.66 eV contains ionizations from two molecular orbitals with similar orbital character: C 2s

from both types of C and σ(P-OCH_3). A large contribution from the σ(P-CH_3) bond and the methoxy C 2s atomic orbitals to the ionization at 23.98 eV was found. Figure S3 shows the correlation of the calculated Kohn-Sham orbital energies with the ionizations in the valence spectrum and molecular orbital plots of all orbitals.

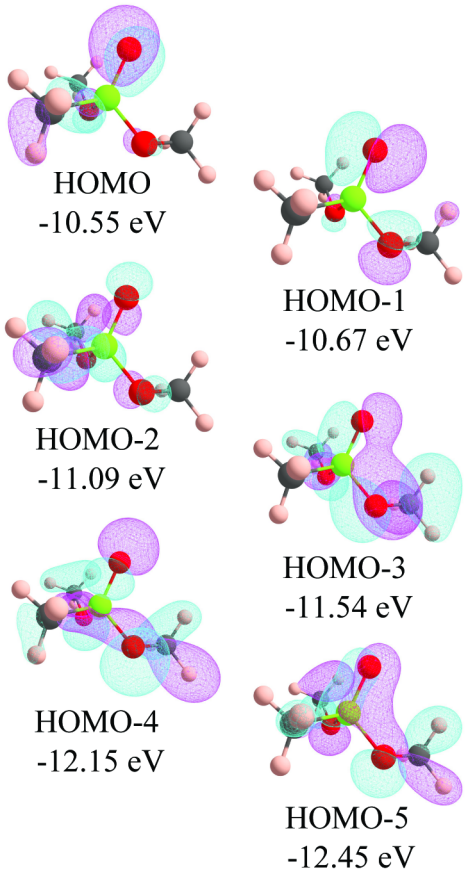

Figure 4. Molecular orbital plots of DMMP and Kohn-Sham orbital energies.

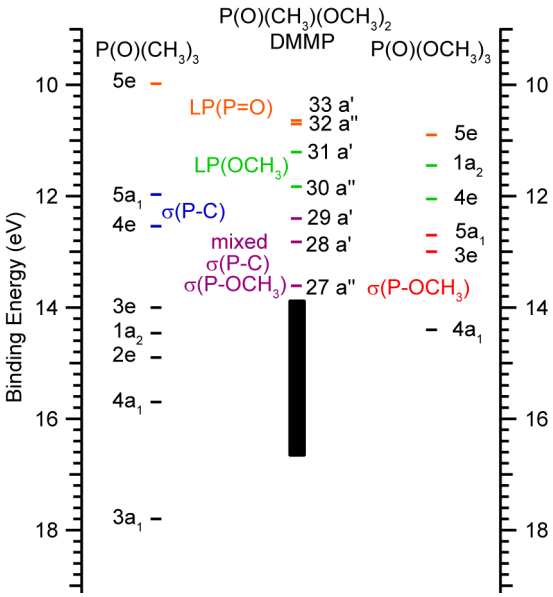

Figure 5. Correlation diagram of the experimental ionization energies of the molecular orbitals in trimethyl phosphine oxide [$P(O)(CH_3)_3$], DMMP, and trimethyl phosphate [$P(O)(OCH_3)_3$]. The atomic origin of the molecular orbitals are color-coded. The black rectangle represents the overlapping ionizations of DMMP described in the text. Values for $P(O)(CH_3)_3$ and $P(O)(OCH_3)_3$ are taken from Ref. [17] and Ref. [18], respectively.

Unoccupied Molecular Orbitals

To gain insight into the unoccupied orbitals of DMMP, the gas-phase NEXAFS spectra were collected of the C and O K-edges and are displayed in Figures 6a and 6b, respectively. TD-DFT calculations were performed to simulate the spectra and assign transitions. In the C K-edge spectrum, the first transition to the lowest unoccupied molecular orbital (LUMO) originates from the methyl C 1s level. The next peak at 288.1 eV correlates with the C_{POCH3} → LUMO transition. Select transitions are labelled in Table 4 and show that the spectrum is dominated by mixed valence/Rydberg transitions that become closer in energy until the ionization threshold, marked by blue dashed lines in Figure 6. The Rydberg transitions originating from the methyl carbon and methoxy carbon atoms overlay each other. In contrast, the beginning of the O K-edge spectrum

contains only transitions from the phosphoryl oxygen. Transition 7 in Figure 6b is the first transition from the O1s of the methoxy O atom to the LUMO.

Taking into consideration that the unoccupied orbitals are rather delocalized (Figure S5), we calculated C K-edge and O K-edge spectra of DMMP using Ahlrichs's TZVP basis set expanded by Pople's (TZVP++) and Dunning's (aug-TZVP) diffuse functions. We found that an addition of the diffuse functions does not improve agreement between calculated and experimental spectra. On the contrary, spectra obtained with TZVP++ and aug-TZVP basis sets are in worse agreement with experimentally measured spectra (Figures S6).

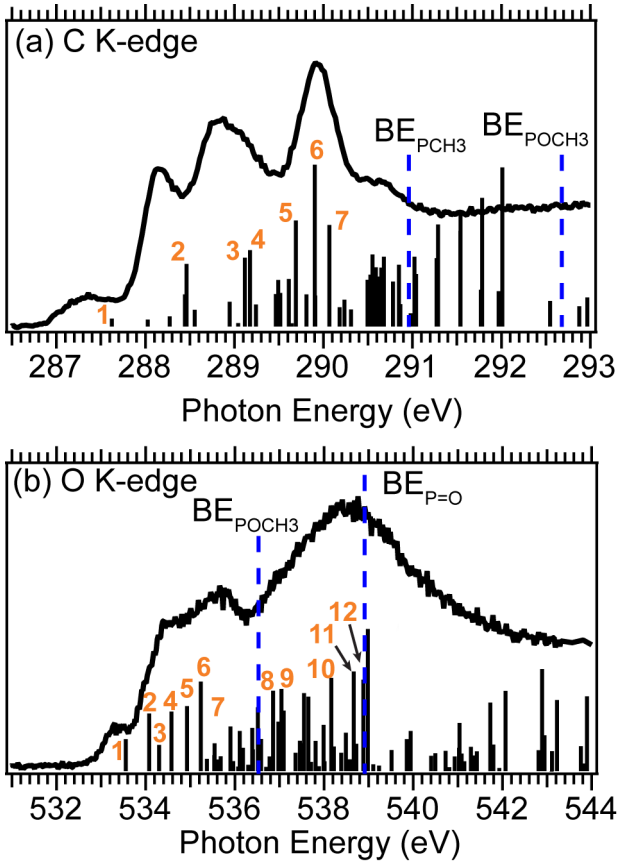

Figure 6. The NEXAFS spectra of the (a) C K-edge and (b) O K-edge of DMMP. The blue vertical lines are the experimental binding energies of the indicated atom. The black vertical lines are calculated transitions, with the intensities corresponding to oscillator strengths. The calculated values have been shifted by 17.52 eV in the C spectrum and by 6.75 eV in the O spectrum.

Table 4. Assignments of the labeled transitions in the NEXAFS spectra in Figure 6.

	label	Transition	orbital
C K-edge	1	C_{PCH3} □ P(*s*) + $C_{P\text{-}CH3}$(*s*) + $H_{P\text{-}CH3}$(*s*)	LUMO
	2	C_{OCH3} □ P(*s*) + $C_{P\text{-}CH3}$(*s*) + $H_{P\text{-}CH3}$(*s*)	LUMO
	3	$C_{O\text{-}CH3}$(1*s*) □ P(*p*) + $C_{O\text{-}CH3}$(*s*) + H(*s*)+$O_{O\text{-}CH3}$(*s*)	LUMO+1
	4	$C_{P\text{-}CH3}$(1*s*) □ P(*s*) + $C_{P\text{-}CH3}$(*s*) + C_{OCH3}(*s*) + H(*s*)	LUMO+5
	5	$C_{P\text{-}CH3}$(1*s*) □ $C_{O\text{-}CH3}$(*p*)+H(*s*)	LUMO+8
	6	$C_{P\text{-}CH3}$(1*s*) □ P(*p*)+$C_{P\text{-}CH3}$(*p*)+H(*s*)	LUMO+9
	7	$C_{P\text{-}CH3}$(1*s*) □ P(*p*)+$C_{P\text{-}CH3}$(*p*)+H(*s*)	LUMO+10
O K-edge	1	$O_{P\text{-}O}$(1*s*) □ P(*s*) + $C_{P\text{-}CH3}$(*s*) + $H_{P\text{-}CH3}$(*s*)	LUMO
	2	$O_{P=O}$(1*s*) □ P(*p*) + $C_{O\text{-}CH3}$(*s*) + H(*s*)+$O_{O\text{-}CH3}$(*s*)	LUMO+1
	3	$O_{P=O}$(1*s*) □ P(*p*) + $C_{P\text{-}CH3}$(*s*) + H(*s*) + $C_{O\text{-}CH3}$(*s*) + $C_{O\text{-}CH3}$(*p*)	LUMO+2
	4	$O_{P=O}$(1*s*) □ P(*p*) + $C_{P\text{-}CH3}$(*s*) + $C_{O\text{-}CH3}$(*s*) + H(*s*)	LUMO+3
	5	$O_{P=O}$(1*s*) □ P(*p*) + $C_{P\text{-}CH3}$(*s*) + $C_{O\text{-}CH3}$(*s*) + H(*s*)	LUMO+4
	6	$O_{P=O}$(1*s*) □ P(*p*) + $C_{P\text{-}CH3}$(*s*) + $C_{O\text{-}CH3}$(*s*) + H(*s*)	LUMO+5
	7	$O_{O\text{-}CH3}$(1*s*) □P(*s*) + $C_{P\text{-}CH3}$(*s*) + H(*s*)	LUMO
	8	$O_{P=O}$(1*s*) □ P(*p*) + H(*s*)	LUMO+13
	9	$O_{P=O}$(1*s*) □ P(*p*) + H(*s*)	LUMO+14
	10	$O_{O\text{-}CH3}$(1*s*) □$C_{P\text{-}CH3}$(*s*) +$C_{O\text{-}CH3}$(*s*) + H(*s*)	LUMO+11
	11	$O_{O\text{-}CH3}$(1*s*) □ P(*p*) + H(*s*)	LUMO+13
	12	$O_{O\text{-}CH3}$(1*s*) □ P(*p*) + H(*s*)	LUMO+14

Conclusions

To gain a thorough description of the electronic structure of DMMP, gas-phase photoelectron and NEXAFS spectroscopy studies were performed. The C and O K-edge NEXAFS spectra were found to be dominated by transitions to mixed valence/Rydberg states. Comparing both the valence and core-level spectra with those of the parent molecules trimethyl phosphate and trimethyl phosphine oxide, classic binding energy shifts with functional group substitution on the P atom were observed. Kohn-Sham orbital energies and partial density of states from DFT calculations were used to assign the valence photoelectron spectrum with more detail than a previous report.[18] The calculations agree well with the spectroscopy results, and the DFT functionals will be used for further studies on DMMP reactivity and CWA properties. Though it

is beyond the scope of this work, the DFT calculations lay the foundation for the computation of other spectra such as UV and vacuum UV absorption spectra.

These spectra provide a reference of the isolated molecule and can be used to interpret spectra of DMMP adsorbed to surfaces, an area of interest for studying materials for, e.g. CWA sensing and destruction. Previously, the assignment of a valence spectrum of a multilayer of DMMP on a Rh(100) surface[42] was found to be too complex to fit, likely due to DMMP decomposition on the surface. With the greater availability of synchrotron light sources for such surface studies, better resolution can be attained, as demonstrated in this work. Moreover, the photon energy can be changed to take advantage of differing photoionization cross sections of elements. With the concrete assignment of our more resolved gas-phase valence spectrum, interpretation of DMMP adsorbed onto a surfaces could be more easily performed. Additionally, UV photoelectron spectroscopy (UPS) is often used to study the electronic structure of interfaces of electronic device materials where monolayers of organophosphonates have been used to tune energy levels.[1] A library of gas-phase valence spectra of these molecules can aid in the interpretation of these UPS studies and build a knowledge base of which functional groups are needed in the organophosphonate to produce desired changes in energy levels.

ASSOCIATED CONTENT

Supporting Information. Additional molecular orbital plots, optimized molecular structure coordinates, and fit parameters of the core level photoelectron spectra. This material is available free of charge via the Internet at http://pubs.acs.org.

AUTHOR INFORMATION

Corresponding Author

* mkukla@umd.edu, 301-405-0221 (M.M.K.); hbluhm@lbl.gov, 510-486-5431 (H.B.)

Notes

The authors declare no competing financial interest.

ACKNOWLEDGMENT

This work was funded by the Department of Defense (Grant HDTRA11510005). R.T. and M.M.K acknowledge support from NSF XSEDE resources (Grant DMR-130077) and DOE NERSC resources (Contract DE-AC02-05CH11231). Osman Karslıoğlu and Matthias Hartl are thanked for their assistance with data collection. MMK is grateful to the Office of the Director of National Science Foundation for support under the Independent Research and Development program. Any appearance of findings, conclusions, or recommendations expressed in this material are those of the authors and do not necessarily reflect the views of NSF.

ABBREVIATIONS

BE, binding energy; CWA, chemical warfare agent; DFT, density functional theory; DOS, density of states; DMMP, dimethyl methylphosphonate; FWHM, full width at half-maximum; HOMO, highest occupied molecular orbital; LP, lone pair of electrons; LUMO, lowest unoccupied molecular orbital; NEXAFS, near-edge X-ray fine structure; PDOS, partial density of states; TD-DFT, time-dependent density functional theory; UPS, UV photoelectron spectroscopy.

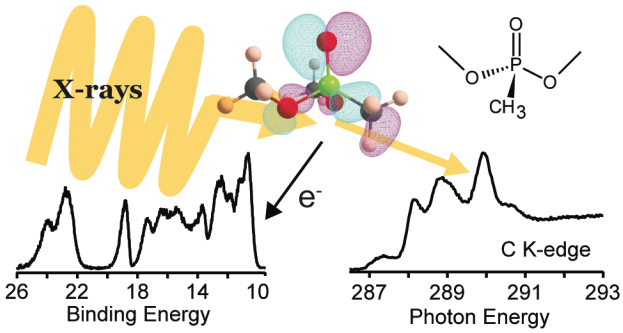
X-rays
e-
O
P
O
O
CH3
C K-edge
26
22
18
14
10
Binding Energy
287
289
291
293
Photon Energy

References

[1] Timpel, M.; Nardi, M. V.; Ligorio, G.; Wegner, B.; Pätzel, M.; Kobin, B.; Hecht, S.; Koch, N. Energy-Level Engineering at ZnO/Oligophenylene Interfaces with Phosphonate-Based Self-Assembled Monolayers. *ACS Appl. Mater. Interfaces* **2015**, *7*, 11900-11907.

[2] Maxisch, M.; Thissen, P.; Giza, M.; Grundmeier, G. Interface Chemistry and Molecular Interactions of Phosphonic Acid Self-Assembled Monolayers on Oxyhydroxide-Covered Aluminum in Humid Environments. *Langmuir* **2011**, *27*, 6042-6048.

[3] Kim, K.; Tsay, O. G.; Atwood, D. A.; Churchill, D. G. Destruction and Detection of Chemical Warfare Agents. *Chem. Rev.* **2011**, *111*, 5345-5403.

[4] Yang, L.; Shroll, R. M.; Zhang, J.; Lourderaj, U.; Hase, W. L. Theoretical Investigation of Mechanisms for the Gas-Phase Unimolecular Decomposition of DMMP. *J. Phys. Chem. A* **2009**, *113*, 13762–13771

[5] Liang, S.; Hemberger P.; Neisius, N. M.; Bodi, A., Grützmacher, H.; Levalois-Grützmacher, J.; Gaan, S. Elucidating the Thermal Decomposition of Dimethyl Methylphosphonate by Vacuum Ultraviolet (VUV) Photoionizatoin: Pathways to the PO Radical, a Key Species in Flame-Retardant Mechanisms. *Chem. Eur. J.* **2015**, *21*, 1073-1080.

[6] Bermudez, V. M. Computational Study of Environmental Effects in the Adsorption of DMMP, Sarin, and VX on γ-Al2O3: Photolysis and Surface Hydroxylation. *J. Phys. Chem. C* **2009**, *113*, 1917–1930

[7] Bermudez, V. M. Computational Study of the Adsorption of Dimethyl Methylphosphonate (DMMP) on the (010) Surface of Anatase TiO_2 With and Without Faceting. *Surf. Sci.* **2010**, *604*, 706–712

[8] Bermudez, V. M. Quantum-Chemical Study of the Adsorption of DMMP and Sarin on γ-Al_2O_3. *J. Phys. Chem. C* **2007**, *111*, 3719-3728.

[9] Zhanpeisov, N. U.; Zhidomirov, G. M.; Yudanov, I. V. Cluster Quantum Chemical Study of the Interaction of Dimethyl Methylphosphonate with Magnesium Oxide. *J. Phys. Chem.* **1994**, *98*, 10032-10035.

[10] Yang, Li; Taylor, R. ; de Jong, W. A.; Hase, W. L. A Model DMMP/TiO_2 (110) Intermolecular Potential Energy Function Developed from *ab Initio* Calculations. *J. Phys. Chem. C* **2011**, *115*, 12403–12413.

[11] Quenneville, J.; Taylor, R. S.; van Duin, A. C. T. Reactive Molecular Dynamics Studies of DMMP Adsorption and Reactivity on Amorphous Silica Surfaces. *J. Phys. Chem. C* **2010**, *114*, 18894–18902

[12] Ahmadian, N.; Ganji, M. D.; Laffafchy M. Theoretical Investigation of Nerve Agent DMMP Adsorption onto Stone-Wales Defected Single-Walled Carbon Nanotube. *Mater. Chem. Phys.* **2012**, *135*, 569-574

[13] Ganji, M. D.; Dalirandeh, Z.; Khosravi, A.; Fereidoon, A. Aluminum Nitride Graphene for DMMP Nerve Agent Adsorption and Detection. *Mater. Chem. Phys.* **2014**, *145*, 260-267

[14] Sodhi, R. N.; Cavell, R. G. KLL Auger and Core-level (1s and 2p) Photoelectron Shifts in a Series of Gaseous Phosphorus Compounds. *J. Electron Spectrosc. Relat. Phenom.* **1983,** *32,* 283-312.

[15] Hohlneicher, G.; Pulm, H. On the Separation of the Initial and Final State Effects in Photoelectron Spectroscopy Using an Extension of the Auger-parameter Concept. *J. Electron Spectrosc. Relat. Phenom.* **1995**, *37*, 209-224.

[16] Elbel, S.; tom Dieck, H. Photoelectron Spectra of Group 5 Compounds. Part IV. A Study of the E-X Bond in R_3EX Compounds (R = Me or F; E = N or P; X = O or S). *J. Chem. Soc., Dalton Trans.* **1976**, 1757-1762.

[17] Vovna, V. I., Okhota, B. V.; Alekseiko, L. N.; Prikhod'ko, Yu. V. Photoelectron Spectra of Trialkylphosphine Oxides. *J. Struct. Chem.* **1990,** *33,* 52-57.

[18] Chattopadhyay, S.; Findley, G. L.; McGlynn, S. P. Photoelectron Spectroscopy of Phosphites and Phosphates. *J. Electron Spectrosc. Relat. Phenom.* **1981**, *24*, 27-36.

[19] Perry, W. B.; Schaaf, T. F.; Jolly, W. L. X-ray Photoelectron Spectroscopic Study of Charge Distributions in Tetracovalent Compounds of Nitrogen and Phosphorus. *J. Am. Chem. Soc.* **1975**, *97,* 4899-4905.

[20] Avanzino, S. C.; Jolly, W. L.; Lazarus, M. S.; Perry, W. B.; Rietz, R. R.; Schaaf, T. F. Evidence for Hyperconjugation from an X-ray Photoelectron Spectroscopic Study of Isoelectronic Conmpounds. *Inorg. Chem.* **1975,** *14*, 1595-1597.

[21] Jolly, W. L. Bomben, K. D.; Eyermann, C. J. Core-electron Binding Energies for Gaseous Atoms and Molecules. *At. Nuc. Data Tables* **1984**, *31*, 433-493.

[22] Li, H.; Hua, W.; Lin, A.; Luo, Y. First-Principles Study on Core-level Spectroscopy of Arginine in Gas and Solid Phases. *J. Phys. Chem. B* **2012,** *116*, 12641-12650.

[23] Olivieri, G.; Cossaro, A.; Capria, E.; Benevoli, L.; Coreno, M.; De Simone, M.; Prince, K. C.; Kladnik, G.; Cvetko, D.; Fraboni, B. et al. Intermolecular Hydrogen Bonding and Molecular

Orbital Distortion in 4-Hydroxycyanobenzene Investigated by X-ray Spectroscopy. *J. Phys. Chem. C*. **2015**, *119,* 121-129.

[24] Ogletree, D. F.; Bluhm, H.; Hebenstreit, E. D.; Salmeron, M. Photoelectron Spectroscopy Under Ambient Pressure and Temperature Conditions. *Nucl. Instrum. Methods Phys. Res., Sect. A* **2009***, 601*, 151-160.

[25] Bluhm, H.; Andersson, K.; Araki, T.; Benzerara, K.; Brown, G. E.; Dynes, J. J.; Ghosal, S.; Gilles, M. K.; Hansen, H.-Ch.; Hemminger, J. C.; et al. Soft X-ray Microscopy and Spectroscopy at the Molecular Environmental Science Beamline at the Advanced Light Source. *J. Electron Spectrosc. Relat. Phenom.* **2006***, 150*, 86-104.

[26] Edqvist, O.; Lindholm, E.; Selin, L. E.; Åsbrink, L. On the Photoelectron Spectrum of O_2. *Phys. Scr.* **1970***, 1*, 25.-30

[27] Larsson, M.; Baltzer, P., Svensson, S.; Wannberg, B.; Mårtensson, N.; Naves de Brito, A.; Correia, N.; Keane, M. P.; Carlsson-Göthe, M.; Karlsson, L. X-ray Photoelectron, Auger Electron and Ion Fragment Spectra of O_2 and Potential Curves of O_2^{2+}. *J. Phys. B.: At. Mol. Opt. Phys.* **1990,** *23,* 1175-1195.

[28] Lichtenberger, D. L.; Copenhaver, A. S. Ionization Band Profile Analysis in Valence Photoelectron Spectroscopy. *J. Electron Spectrosc. Relat. Phenom.* **1990***, 50*, 335-352.

[29] Frisch, M. J.; Trucks, G. W.; Schlegel, H. B.; Scuseria, G. E.; Robb, M. A.; Cheeseman, J. R.; Scalmani, G.; Barone, V.; Mennucci, B.; Petersson, G. A.; et al. Gaussian 09, revision B.01;Gaussian, Inc.: Wallingford, CT, 2010.

[30] Zhao, Y.; Truhlar, D. G. The M06 Suite of Density Functionals for Main Group Thermochemistry, Thermochemical Kinetics, Noncovalent Interactions, Excited States, and

Transition Elements: Two New Functionals and Systematic Testing of Four M06-class Functionals and 12 Other Functionals. *Theor. Chem. Acc.* **2008**, *120*, 215-241.

[31] O'boyle, N. M.; Tenderholt, A. L.; Langner, K. M. cclib: A Library for Package-independent Computational Chemistry Algorithms. *J. Comput. Chem.* **2008**, 29, 839–845.

[32] Neese, F.; Olbrich, G. Efficient Use of the Resolution of the Identity Approximation in Time-Dependent Density Functional Calculations with Hybrid Density Functionals. *Chem. Phys. Lett.* **2002**, *362*, 170–178.

[33] Becke, A. D. Density-functional Exchange-energy Approximation with Correct Asymptotic Behavior. *Phys. Rev. A* **1988**, *38*, 3098-3100.

[34] Perdew, J. P. Density-functional Approximation for the Correlation Energy of the Inhomogeneous Electron Gas. *Phys. Rev. B* **1986**, *33*, 8822-24.

[35] Schäfer, A.; Horn, H.; Ahlrichs, R. Fully Optimized Contracted Gaussian-basis Sets for Atoms Li to Kr. *J. Chem. Phys.* **1992**, *97*, 2571-2577.

[36] Schäfer, A.; Huber, C.; Ahlrichs, R. Fully Optimized Contracted Gaussian-basis Sets of Triple Zeta Valence Quality for Atoms Li to Kr. *J. Chem. Phys.* **1994**, *100*, 5829-35.

[37] Neese, F. The ORCA Program System. *Wiley Interdiscip. Rev.: Comput. Mol. Sci.* **2012**, *2*, 73-78.

[38] DeBeer George, S.; Petrenko, T.; Neese, F. Prediction of Iron K-Edge Absorption Spectra Using Time-Dependent Density Functional Theory. *J. Phys. Chem. A* **2008**, 112, 12936–12943.

[39] DeBeer George, S.; Petrenko, T.; Neese, F. Time-dependent Density Functional Calculations of Ligand K-edge X-ray Absorption Spectra. *Inorg. Chim. Acta* **2008**, *361*, 965-972.

[40] Suenram, R. D.; Lovas, F. J.; Plusquellic, D. F.; Lesarri, A.; Kawashima, Y.; Jensen, J. O.; Samuels, A. C. Fourier Transform Microwave Spectrum and *ab Initio* Study of Dimethyl Methylphosphonate. *J. Mol. Spectrosc.* **2002**, *211*, 110-118.

[41] Griffith, O. L.; Gruhn, N. E.; Anthony, J. E.; Purushothaman, B.; Lichtenberger, D. L. Electron Transfer Parameters of Triisopropylsilylethynyl-Substituted Oligoacenes. *J. Phys. Chem. C* **2008**, *112*, 20518-20524.

[42] Hedge, R. I.; Greenlief, C. M.; White, J. M. Surface Chemistry of Dimethyl Methylphosphonate on Rhodium(110). *J. Phys. Chem.* **1985,** *89,* 2886-2891.